This is a repository copy of *A Patient-specific Wear Prediction Framework for an Artificial Knee Joint with Coupled Musculoskeletal Multibody-dynamics and Finite Element Analysis*.

White Rose Research Online URL for this paper:
http://eprints.whiterose.ac.uk/107688/

Version: Accepted Version

Author's Accepted Manuscript

A Patient-specific Wear Prediction Framework for an Artificial Knee Joint with Coupled Musculoskeletal Multibody-dynamics and Finite Element Analysis

Jing Zhang, Zhenxian Chen, Ling Wang, Dichen Li, Zhongmin Jin
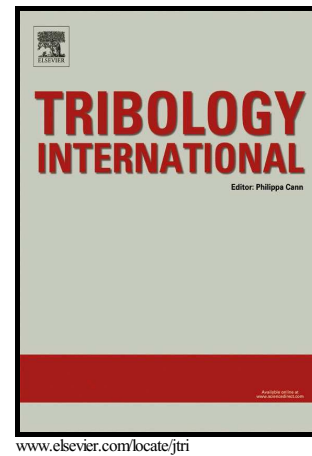
Cite this article as: Jing Zhang, Zhenxian Chen, Ling Wang, Dichen Li and Zhongmin Jin, A Patient-specific Wear Prediction Framework for an Artificial Knee Joint with Coupled Musculoskeletal Multibody-dynamics and Finit Element Analysis, *Tribology International* http://dx.doi.org/10.1016/j.triboint.2016.10.050

A Patient-specific Wear Prediction Framework for an Artificial Knee Joint with Coupled Musculoskeletal Multibody-dynamics and Finite Element Analysis

Jing Zhang[a], Zhenxian Chen[a,*], Ling Wang[a], Dichen Li[a], Zhongmin Jin[a,b,c]

[a]State Key Laboratory for Manufacturing System Engineering, School of Mechanical Engineering, Xi'an Jiaotong University, 710054, Xi'an, Shaanxi, China

[b]Institute of Medical and Biological Engineering, School of Mechanical Engineering, University of Leeds, Leeds, LS2 9JT, UK

[c]Tribology Research Institute, School of Mechanical Engineering, Southwest Jiaotong University, 610031, Chengdu, Sichuan, China

[*]Corresponding author Tel.: +0-86-029-83399056; Ezhenxian_chen@yeah.net

Abstract

A novel wear prediction framework was developed by coupling a patient-specific lower extremity musculoskeletal multibody dynamics model with the finite element contact mechanics and wear model of total knee replacement. The tibiofemoral contact forces and kinematics were influenced by articular surface wear, and in turn, the variations from the knee dynamics resulted in increases in the volumetric wear of 404.41 mm^3 after 30 million cycle simulation from 380.86 mm^3 from the traditional wear prediction using fixed load/motions. The developed patient-specific wear prediction framework provided a reliable virtual platform for investigating articular surface wear of total knee replacements.

Keywords: Wear prediction, Finite-element method, Musculoskeletal multibody dynamics, Total knee replacement

1. Introduction

Total knee replacement (TKR) is effective to replace the damaged cartilage tissues and help the patients to restore daily activities [1]. Although the survivorship of knee implants may extend beyond two decades [2], wear debris of ultra-high molecular weight polyethylene (UHMWPE) in TKR induced aseptic loosening is still a major limitation to longevity [3-6]. Laboratory knee wear simulator testing is invaluable for understanding polyethylene wear mechanisms and pre-clinically evaluating new implant designs and materials [7-14]. However, the experimental testing is associated with substantial cost and time, as a large number of low frequency gait cycles are required [8, 15], while computational wear modeling is an alternative attractive solution [1, 16].

Patient-specific load/kinematics play an important role in vivo wear behavior [6, 17], however, the majority of previous computational wear studies [1, 15, 18, 19] have adopted the load/motions specified in ISO 14243 (2009) [20] as the input condition. Although some studies [21] have adopted a patient-specific kinematics, the load was not from the same patient. In vivo contact forces and joint motions are essential for patient-specific wear prediction [6]. Although in vivo knee contact forces

and joint motions have been measured using instrumented knee prostheses [22, 23] and fluoroscopic imaging system [24] respectively, it is still difficult to obtain all these information from the same patient simultaneously. Consequently, multibody dynamics (MBD) modelling of TKR by considering the patient-specific lower extremity musculoskeletal (MSK) system is an alternative attractive method to the in vivo measurements [25-27].

The patient-specific lower extremity MSK MBD models of TKR [25-27] have been established to predict the tibiofemoral joint forces and secondary knee kinematics with a reasonably good accuracy, based on the elastic foundation model [28] which incorporate a deformable knee implant into a rigid MBD simulation [29], and the force-dependent kinematics (FDK) method [27] for predicting the secondary motions. The predicted in vivo knee joint forces and motions can readily be used to predict the surface wear of the TKR using the methodology already established [1]. All previous wear predictions have used fixed load/kinematics for the wear simulation of TKR, and not considered the effect of the change of kinematics/load due to tibial insert geometry variation caused by wear [30-33]. The use of fixed load/motion in the wear simulation means that the change of these input conditions, which affects the multi-directional cross-shear motion [34, 35], has not been considered. It is feasible to predict the implant wear under the patient-specific load/kinematics condition by coupling a lower extremity MSK MBD model implanted with specific knee prosthesis, with the contact mechanics model and wear model. However, to our knowledge, such a framework has not been reported.

This study aimed to develop a novel patient-specific computational wear prediction framework of TKR by coupling a lower extremity MSK MBD model implanted with a specific knee prosthesis, the contact mechanics model and wear model. Furthermore, the interaction between the knee joint load and motions, contact stress and wear of the bearing surface in the TKR was investigated.

2. Materials and methods

2.1 Patient-specific musculoskeletal model

A patient-specific lower extremity MSK model which was validated for the joint load in our previous study [25, 26] was used in this study. The patient-specific MSK model was developed in Anybody (version 6.0; AnyBody Technology, Aalborg,

2

Denmark) using publically available data (https://simtk.org/home/kneeloads) [36], collected from a specific patient (subject PS, male, 180cm, 75kg) implanted with an instrumented knee implant. The generic lower extremity MSK model (AnyBody Managed Model Repository V1.6.2), which is based on the Twente Lower Extremity Model [37] anthropometric database, was scaled to the patient-specific MSK model according to the patient pre-operative bone geometries using an advanced bone morphing method [38]. Meanwhile, all related muscle and ligament attachment points or areas defined on the given bone were scaled accordingly to match the patient bone geometries. The patient post-operative bones with the instrumented Zimmer NK-II cruciate-retaining prosthesis were rigidly registered to the scaled femur and tibia. A new knee joint model with 11 degrees of freedoms was developed, based on the FDK method [39], which included deformable contact surfaces and ligaments. The soft tissues crossing the tibial-femoral (TF) and patella-femoral (PF) joint included the medial collateral ligament (MCL), the lateral collateral ligament (LCL), the posterior cruciate ligament (PCL), the posteromedial capsule (PMC), and the medial and lateral PF ligaments (MPFL, LPFL). Ligaments were modeled as non-linear spring elements with a piecewise force–displacement relationship [40]. Three contact pairs were defined between the medial and lateral of the tibial insert and the femoral component and between the patellar button and the femoral component based on the elastic foundation theory [29]. The UHMWPE was considered as a non-linear material [25]. All contact forces between the contacting surfaces were calculated using a linear force-penetration volume law with a contact PressureModule of 1.24×10^{11} N/m^3 in this study [41]; further details can be found in a previous study [25].

The patient's standing reference trial used to scale the other remaining segments and determine original model marker locations, and a patient-specific walking gait trial with experimental ground reaction forces were imported into the developed MSK model to calculate the medial, lateral and total TF contact forces, PF contact force and ligament forces, as well as the knee joint motions using the FDK solver during a simulated walking gait [25].

2.2 Finite element model

A finite element (FE) model (Fig. 1) of the corresponding TKR of the above patient was developed using Abaqus/Explicit (Abaqus 6.12, Simulia Inc., Providence, RI) to calculate the contact mechanics. The tibial insert was modeled as a non-linear

3

material with a modulus of elasticity of 463 MPa and a Poisson's ratio of 0.46 [1]. The tibial insert and the femoral component were meshed using linear hexahedral elements (C3D8I) and quadratic tetrahedral elements (C3D10M) respectively. Mesh densities were determined by convergence studies, which resulted in an approximate global size of 1.0 mm for the insert, 1.5 mm for the femoral component. A penalty contact was defined between the contact surfaces，including a coefficient of friction of 0.04, and this value was in accordance with artificial joints and experimental pin-on-disk (POD) tests, as well as previous computational models [42-45].

The outputs from the gait simulation of the patient-specific lower extremity MSK model were used as the boundary conditions (BCs) for the developed FE model. The total contact force was applied on the reference node of the femoral component, defined at the axis through the center of the femoral contact surface and offset 5 mm in the medial direction, according to ISO 14243 [20]. The flexion-extension of the femoral component was also prescribed through the reference node (Fig. 1b). The adduction–abduction motion was left free. All other degrees of freedom of the femoral component were constrained. Anterior-posterior displacement and internal-external rotation were applied on the tibial reference node. All other degrees of freedom of the tibial insert were constrained.

2.3 Wear model

In this study, the model developed and validated by Abdelgaied et al. [1] was adopted to predict the articular surface wear of the UHMWPE tibial insert in the presence of bovine serum lubricant. This wear model was used widely in wear prediction [1, 46, 47]. The wear model was based on the idea that wear volume (V) is proportional to the contact area (A) and sliding distance (S):

$$V = CAS \tag{1}$$

where C is a non-dimensional wear coefficient dependent on a cross-shear ratio (CS), determined from the experimental measurements of a multi-directional POD wear test in the presence of bovine serum lubricant to achieve the same boundary and mixed lubrication condition as in artificial joints [35, 48-50]:

$$C = (a + b \times CS)^{-1/c} \tag{2}$$

where a, b and c are constants, and the CS was defined on the unified theory of wear and work [34, 35, 51], as the component of the frictional work perpendicular to the principal molecular orientation direction ($E_{cross-shear}$), divided by the total frictional work (E_{total}):

$$CS = \frac{E_{cross-shear}}{E_{total}} \tag{3}$$

The effect of UHMWPE creep was also considered, based on the experimental data reported [52]. The creep was modeled as:

$$\delta_{creep} = [3.491 \times 10^{-3} + 7.966 \times 10^{-4}(\log(t) - 4)]\sigma_{av}h \tag{4}$$

where t is time (min), σ_{av} is the average pressure (MPa), and h is the thickness (mm).

The total linear damage (δ_{total}) of each node on the insert surface, which was the sum of linear wear (δ_{wear}) and creep deformation (δ_{creep}), was used to update the surface geometry:

$$\delta_{total} = \delta_{wear} + \delta_{creep} \tag{5}$$

2.4 Coupling prediction framework

A novel computational framework was established by coupling the above patient-specific MSK model, FE model and wear model of the knee implant (Fig. 2). The patient-specific MSK MBD model of the TKR calculated joint forces/motions during gait simulation, then these were input into the FE model as the BCs to calculate the contact pressure and sliding distances of the insert at each node and each time increment. Custom Python scripts were used to extract the results from Abaqus output database, and a Matlab script was developed to calculate wear and creep for each node of the contact surfaces and output the worn insert geometry. The updated worn insert geometry was subsequently imported into the MSK MBD model to calculate new joint load/motions for the new FE analysis. The insert surface was updated, using the total linear damage depth at each node. Two iterations were performed for the first 1 million cycles, to account for the large creep at the early stage, and then every 2 million cycles were considered till 30 million cycles. A non-coupled wear model with the constant BCs as the initial gait cycle for the whole simulation was also considered for the purpose of comparison.

5

3. Results and discussion

3.1 Musculoskeletal model

Fig. 3 shows the effect of the articular surface wear on the knee joint contact forces and motions during a 30 million cycle simulation. The insert wear changed the TF lateral-medial load distribution. The lateral contact force (Fig. 3a) increased during the stance phase, especially at 20% gait cycle, the amplitude increased by 17.76% and 33.22% after 20 million cycle and 30 million cycles respectively. At the meantime, the medial contact force (Fig. 3b) decreased, and the second crest decreased by 2.99% and 7.50% after 20 million cycle and 30 million cycles respectively. The effect of wear on the total contact force (Fig. 3c) was slight, and the second peak decreased by 3.08% and 5.88% after 20 million cycle and 30 million cycles respectively. For the joint motions, the primary flexion-extension motion (Fig. 3d) was not sensitive to the wear. However, relatively larger changes were found in the secondary knee kinematics, especial the anterior-posterior translation (Fig. 3e) and the internal-external rotation (Fig. 3f). Compared with the initial values, the range of the anterior-posterior translation of the femoral component decreased 14.43% after 30 million cycles. The amplitude of the femoral external rotation increased especially during the stance phase of the gait cycle with a peak increase of 7.52% after 30 million cycles wear. Williams et al. [53] investigated how the wear changed kinematics and contact stresses using a retrieved polyethylene insert of TKR. They found the worn articular surface resulted in a decrease in the range of anterior-posterior translation and an increase in femoral external rotation. Our findings were consistent with their results, although the percentage changes were different.

The effects of the wear on the ligament forces are shown in Fig. 4. The PCL and LCL forces were not sensitive to the wear. The PCL was slightly increased during the stance phase, while the LCL was slightly decreased during the swing phase. The MCL force had a relatively large decrease of 18.84% after 30 million cycles during the stance phase. In this study, the wear of articulating surfaces resulted in the geometry change of the tibial insert, and this further influenced the muscle/ligaments moment arms, which directly contributed to the change of the muscle/ligaments forces, eventually leading to the changes in the knee joint forces and motion. The linear wear of the medial side was larger than the lateral side as wear progressed, which increased the laxity of MCL, and the MCL force decreased meanwhile the LCL force slightly increased (Fig.

4). The changes of MCL and LCL eventually altered the TF medial-lateral load distribution and the femoral external rotation. Although the PCL force decreased along with wear, the range of the anterior-posterior translation was not increased, which was mainly restricted by the worn surface.

3.2 Finite element model

Fig. 5 shows the contact pressure distribution at the maximum load of the gait cycle. Generally, for both coupled and non-coupled model, the contact pressure decreased as wear progressed, as a result of the increased contact area, due to the increased conformity. After 5 million cycles, the predicted maximum contact pressure of the non-coupled model was in general steady with slightly increased at some instances, due to the change of the contact surfaces as wear progressed. While for coupled model, the maximum value oscillated, especially at 10 million cycles, for the change of the TF contact force, the anterior-posterior translation and internal-external rotation which subsequently altered the contact location. Both wear and kinematics have combined effect on contact surface change, leading the fluctuation of maximum contact pressure for coupled model. Compared with the non-coupled model, a larger maximum contact pressure was predicted from the coupled model after 5 million cycles, although the differences were small. This is mainly due to the change of the contact surfaces as a result of both kinematics and wear, decreasing the conformity in part of the contact surface compared with the non-coupled model. The maximum contact pressure of the coupled model was transferred from the medial to the lateral side of the insert, apparently after 20 million cycles wear simulation, because of the decreased medial contact force and increased lateral contact force during the stance phase. Williams et al. predicted the peak contact stress increased threefold using a retrieved insert [53], while the maximum contact pressure was slightly decreased in our study. The retrieved insert from Williams et al. was worn severely, and the rough surface caused stress concentration which led to increase in the peak contact stress. However, our study was based on a mild surface wear mechanism [1, 43], which resulted a smooth worn surface. Therefore, the maximum contact pressure did not increase but decrease along with the increasing conformity as the wear simulation continued.

Fig. 6 shows the effect of the variation of knee dynamics on the average contact area (Fig. 6a) during a gait cycle and the average cross-shear ratio (Fig. 6b). Generally, the contact area increased for both models as the wear progressed, with a marked

7

increase from the beginning to 1 million cycles due to the effect of creep. Compared with the non-coupled model, a larger average contact area and average cross-shear ratio were found from the coupled model, mainly due to the change of the anterior-posterior translation and internal-external rotation. The larger average contact area may lead to a smaller average contact pressure, however the maximum value was determined by the change of the contact surfaces as explained above.

3.3 Wear model

The distributions of the accumulated sliding distance of the insert surface for the coupled (Fig. 7a) and non-coupled model (Fig. 7b) are shown in Fig. 7. For both models, the distribution at the initial stage was apparently different from the latter, and the maximum values decreased while the distributed area increased as wear progressed. Small differences were predicted in the distributions from the two models.

The changes of the volumetric wear (Fig. 8a) and worn area (Fig. 8b) of the TKR at different wear stages are shown in Fig. 8. Compared with the non-coupled model, the volumetric wear predicted by the coupled model was larger. Wear volumes of 380.86 mm^3 and 404.41 mm^3 were predicted from the non-coupled model and the coupled mode respectively after 30 million cycles wear simulation. Worn area (Fig. 8b) was increased for both models as wear progressed, and stabilized after 15 million cycles. Worn areas of 1165.18 mm^2 and 1178.80 mm^2 were predicted from the non-coupled model and the coupled model respectively.

Fig. 9 shows the distributions of the linear wear of the insert surface at different wear stages from the coupled (Fig. 9a) and non-coupled model (Fig. 9b). Both models predicted a deep wear scar around the center of the medial side. The worn scars on the medial side from both models were more anterior compared to the lateral side. There were negligible differences in the linear wear distributions between two models.

The effects of the changes in knee joint load/kinematics on wear prediction were investigated by comparing with the non-coupled model. It is also clear from the distribution of accumulated sliding distance and the linear wear, the change of the kinematics, especially the anterior-posterior translation and the internal-external rotation, mostly influenced the contact location. Compared with the non-coupled model, an increased external rotation of the femur was mainly led to an increase in

8

the cross-shear ratio, further leading to a larger wear volume for the coupled simulation. The difference of volumetric wear between coupled and non-coupled model was not obvious, demonstrating that in a well-designed knee implant with small wear, the change of the kinematics and load due to wear was not remarkable.

3.4 Limitations

Although the developed subject-specific wear prediction framework provided a new method to realistically quantify the in vivo wear of TKR, this study still possessed many limitations. Firstly, the patient-specific lower extremity MSK MBD model did not consider the potential change of the patient's gait due to the wear of the tibial insert. Secondly, only a patient with a single gait trail and one type of knee prosthesis were considered in this study, and the patient-specific difference and various implant designs should be investigated in future work. Thirdly, due to the lack of the relevant patient specific ligament properties, generic values were taken from the literature, and the ligament origin and insertion points were located manually to fit the patient's bone geometries according to anatomic descriptions. Fourthly, although the wear model has been verified with experiments [1, 46, 54], the predicted wear volumes were 31%-45% lower than the experimental results [32], and the experimental simulator results may be even smaller than the retrieved TKR [55]. The improvement of the wear model may provide an even more realistic coupled framework. Fifthly, the total TF contact forces were used as the axial load applied at the reference node of the femur, according to ISO 14243 [20]. The MSK MBD model outputted the medial/lateral contact forces respectively, adduction-abduction motion, and medial-lateral translation. All these input conditions could be used directly in the FE modeling and wear simulation. Furthermore, it is also necessary to consider the adverse conditions [5, 11] when the wear of the tibial insert increased markedly, and the consequent effects on the interaction with the biomechanics of the knee implant. Despite of these limitations, the potential advantages of the coupled patient-specific biomechanics and wear prediction framework are evident.

4. Conclusion

A novel patient-specific wear prediction framework of TKR, coupling the lower extremity MSK MBD model implanted with a specific knee prosthesis, FE model and wear model of the artificial knee joint, was developed to investigate the

interaction between the knee joint load/kinematics and the wear of the insert bearing surface. The articular surface wear of the tibial insert resulted in change of ligament forces, which leading to the change of TF medial-lateral load distribution and kinematics. In turn, the changes of the knee joint dynamics contributed to the further articular surface wear of the insert. Taking the interaction between in vivo kinematic/load, contact mechanics and wear into consideration, this patient-specific coupled framework can provide a more realistic prediction of wear and functional outcomes of knee implant designs.

Conflicts of interest statement

There is no conflict of interest.

Acknowledgements

References

[1] Abdelgaied A, Liu F, Brockett C, Jennings L, Fisher J, Jin Z. Computational wear prediction of artificial knee joints based on a new wear law and formulation. Journal of Biomechanics. 2011;44:1108-16.

[2] Sanders AP, Lockard CA, Weisenburger JN, Haider H, Raeymaekers B. Using a surrogate contact pair to evaluate polyethylene wear in prosthetic knee joints. Journal of Biomedical Materials Research Part B: Applied Biomaterials. 2015:n/a-n/a.

[3] Guo Y, Hao Z, Wan C. Tribological characteristics of polyvinylpyrrolidone (PVP) as a lubrication additive for artificial knee joint. Tribology International. 2016;93:214-9.

[4] Qiu M, Chyr A, Sanders AP, Raeymaekers B. Designing prosthetic knee joints with bio-inspired bearing surfaces. Tribol Int. 2014;77:106-10.

[5] E SF, Shi L, Guo ZG, Liu WM. The recent progress of tribological biomaterials. Biosurface and Biotribology. 2015;1:81-97.

[6] Zhou ZR, Jin ZM. Biotribology: Recent progresses and future perspectives. Biosurface and Biotribology. 2015;1:3-24.

[7] Reinders J, Sonntag R, Kretzer JP. Synovial fluid replication in knee wear testing: an investigation of the fluid volume. J Orthop Res. 2015;33:92-7.

[8] Affatato S, Grillini L, Battaglia S, Taddei P, Modena E, Sudanese A. Does knee implant size affect wear variability? Tribology International. 2013;66:174-81.

[9] Brandt JM, Mahmoud KK, Koval SF, MacDonald SJ, Medley JB. Antimicrobial agents and low-molecular weight polypeptides affect polyethylene wear in knee simulator testing. Tribology International. 2013;65:97-104.

[10] Wimmer MA, Birken L, Sellenschloh K, Schneider E. Damage due to rolling in total knee replacement—The influence of tractive force. Friction. 2013;1:178-85.

10

[11] Saikko V. Effect of shelf versus accelerated aging of UHMWPE on delamination in knee wear simulation. Tribology International. 2014;73:10-6.

[12] Zhang L, Sawae Y, Yamaguchi T, Murakami T, Yang H. Effect of radiation dose on depth-dependent oxidation and wear of shelf-aged gamma-irradiated ultra-high molecular weight polyethylene (UHMWPE). Tribology International. 2015;89:78-85.

[13] Ruggiero A, D'Amato R, Gómez E. Experimental analysis of tribological behavior of UHMWPE against AISI420C and against TiAl6V4 alloy under dry and lubricated conditions. Tribology International. 2015;92:154-61.

[14] Ruggiero A, D'Amato R, Gómez E, Merola M. Experimental comparison on tribological pairs UHMWPE/TIAL6V4 alloy, UHMWPE/AISI316L austenitic stainless and UHMWPE/AL2O3 ceramic, under dry and lubricated conditions. Tribology International. 2016;96:349-60.

[15] Knight LA, Pal S, Coleman JC, Bronson F, Haider H, Levine DL, et al. Comparison of long-term numerical and experimental total knee replacement wear during simulated gait loading. Journal of Biomechanics. 2007;40:1550-8.

[16] Mattei L, Di Puccio F, Ciulli E. A comparative study of wear laws for soft-on-hard hip implants using a mathematical wear model. Tribology International. 2013;63:66-77.

[17] Pal S, Haider H, Laz PJ, Knight LA, Rullkoetter PJ. Probabilistic computational modeling of total knee replacement wear. Wear. 2008;264:701-7.

[18] Willing R, Kim IY. A holistic numerical model to predict strain hardening and damage of UHMWPE under multiple total knee replacement kinematics and experimental validation. Journal of Biomechanics. 2009;42:2520-7.

[19] O'Brien ST, Bohm ER, Petrak MJ, Wyss UP, Brandt J-M. An energy dissipation and cross shear time dependent computational wear model for the analysis of polyethylene wear in total knee replacements. Journal of Biomechanics. 2014;47:1127-33.

[20] International Organization for Standardization. Implants for surgery —Wear of total knee-joint prostheses —Part 3: Loading and displacement parameters for wear-testing machines with displacement control and corresponding environmental conditions for test. 2009.

[21] Fregly BJ, Sawyer WG, Harman MK, Banks SA. Computational wear prediction of a total knee replacement from in vivo kinematics. Journal of Biomechanics. 2005;38:305-14.

[22] Haas BD, Komistek RD, Stiehl JB, Anderson DT, Northcut EJ. Kinematic comparison of posterior cruciate sacrifice versus substitution in a mobile bearing total knee arthroplasty. The Journal of Arthroplasty. 2002;17:685-92.

[23] Dennis DA, Komistek RD, Mahfouz MR. In Vivo Fluoroscopic Analysis Of Fixed-Bearing Total Knee Replacements. Clinical Orthopaedics and Related Research. 2003;410:114-30.

[24] Kozanek M, Hosseini A, Liu F, Van de Velde SK, Gill TJ, Rubash HE, et al. Tibiofemoral kinematics and condylar motion during the stance phase of gait. Journal of Biomechanics. 2009;42:1877-84.

[25] Chen Z, Zhang Z, Wang L, Li D, Zhang Y, Jin Z. Evaluation of a Subject-Specific Musculoskeletal Modeling Framework to Predict Load in Total Knee Arthroplasty. Medical Engineering & Physics. 2016.

[26] Chen Z, Jin Z. Prediction of in-vivo kinematics and contact track of total knee arthroplasty during walking. Biosurface and Biotribology. 2016.

[27] Marra MA, Vanheule V, Fluit R, Koopman BHFJM, Rasmussen J, Verdonschot N, et al. A Subject-Specific Musculoskeletal Modeling Framework to Predict In Vivo Mechanics of Total Knee Arthroplasty. Journal of Biomechanical Engineering. 2015;137:020904.

[28] Bei Y, Fregly BJ. Multibody dynamic simulation of knee contact mechanics. Medical Engineering & Physics. 2004;26:777-89.

[29] Fregly BJ, Bei Y, Sylvester ME. Experimental evaluation of an elastic foundation model to predict contact pressures in knee replacements. Journal of Biomechanics. 2003;36:1659-68.

[30] Willing R, Kim IY. Design optimization of a total knee replacement for improved constraint and flexion kinematics. Journal of Biomechanics. 2011;44:1014-20.

[31] Deen ME, ´a-Fin˜ana MG, Jin Z-M. Effect of ultra-high molecular weight polyethylene thickness on contact mechanics in

total knee replacement. Proceedings of the Institution of Mechanical Engineers, Part H: Journal of Engineering in Medicine. 2006;220:733-42.

[32] Galvin AL, Kang L, Udofia I, Jennings LM, McEwen HMJ, Jin Z, et al. Effect of conformity and contact stress on wear in fixed-bearing total knee prostheses. Journal of Biomechanics. 2009;42:1898-902.

[33] Pianigiani S, Chevalier Y, Labey L, Pascale V, Innocenti B. Tibio-femoral kinematics in different total knee arthroplasty designs during a loaded squat: A numerical sensitivity study. Journal of Biomechanics. 2012;45:2315-23.

[34] Wang A. A unified theory of wear for ultra-high molecular weight. Wear. 2001;248:38-47.

[35] Kang L, Galvin AL, Brown TD, Jin Z, Fisher J. Quantification of the effect of cross-shear on the wear of conventional and highly cross-linked UHMWPE. Journal of Biomechanics. 2008;41:340-6.

[36] Fregly BJ, Besier TF, Lloyd DG, Delp SL, Banks SA, Pandy MG, et al. Grand challenge competition to predict in vivo knee loads. Journal of Orthopaedic Research. 2012;30:503-13.

[37] Horsman K, M. D., Koopman HFJM, van der Helm FCT, Prosé LP, Veeger HEJ. Morphological muscle and joint parameters for musculoskeletal modelling of the lower extremity. Clinical Biomechanics. 2007;22:239-47.

[38] Pellikaan P, van der Krogt MM, Carbone V, Fluit R, Vigneron LM, Van Deun J, et al. Evaluation of a morphing based method to estimate muscle attachment sites of the lower extremity. J Biomech. 2014;47:1144-50.

[39] Andersen, J R. Total knee replacement musculoskeletal model using a novel simulation method for non-conforming joints. In Proceedings of the International Society of Biomechanics conference, International Society of Biomechanics, ISB. 2011: 3–7.

[40] Blankevoort L, Kuiper JH, Huiskes R, Grootenboer HJ. Articular contact in a three-dimensional model of the knee. Journal of Biomechanics. 1991;24:1019-31.

[41] Chen Z, Zhang X, Ardestani MM, Wang L, Liu Y, Lian Q, et al. Prediction of in vivo joint mechanics of an artificial knee implant using rigid multi-body dynamics with elastic contacts. Proceedings of the Institution of Mechanical Engineers, Part H: Journal of Engineering in Medicine. 2014;228:564-75.

[42] Sathasivam S, Walker PS. A computer model with surface friction for the prediction of total knee kinematics. Journal of Biomechanics. 1997;30:177-84.

[43] O'Brien S, Luo Y, Wu C, Petrak M, Bohm E, Brandt JM. Computational development of a polyethylene wear model for the articular and backside surfaces in modular total knee replacements. Tribology International. 2013;59:284-91.

[44] Godest AC, Beaugonin M, Haug E, Taylor M, Gregson PJ. Simulation of a knee joint replacement during a gait cycle using explicit finite element analysis. Journal of Biomechanics. 2002;35:267-75.

[45] Jin Z, Dowson D. Bio-friction. Friction. 2013;1:100-13.

[46] Abdelgaied A, Brockett CL, Liu F, Jennings LM, Jin Z, Fisher J. The effect of insert conformity and material on total knee replacement wear. Proceedings of the Institution of Mechanical Engineers, Part H: Journal of Engineering in Medicine. 2013;228:98-106.

[47] Abdelgaied A, Brockett CL, Liu F, Jennings LM, Fisher J, Jin Z. Quantification of the effect of cross-shear and applied nominal contact pressure on the wear of moderately cross-linked polyethylene. Proceedings of the Institution of Mechanical Engineers, Part H: Journal of Engineering in Medicine. 2012;227:18-26.

[48] Kang L, Galvin AL, Fisher J, Jin Z. Enhanced computational prediction of polyethylene wear in hip joints by incorporating cross-shear and contact pressure in additional to load and sliding distance: Effect of head diameter. Journal of Biomechanics. 2009;42:912-8.

[49] Kennedy FE, Wongseedakaew K, McHugh DJ, Currier JH. Tribological conditions in mobile bearing total knee prostheses. Tribology International. 2013;63:78-88.

[50] Wang A, Essner A, Polineni. VK, Stark. C, Dumbleton. JH. Lubrication and wear of ultrahigh molecular weight polyethylene in total joint replacements. Tribology International. 1998;31:17-33.

[51] Lee RK, Korduba LA, Wang A. An improved theoretical model of orientation softening and cross-shear wear of ultra high molecular weight polyethylene. Wear. 2011;271:2230-3.

[52] Lee K-Y, Pienkowski D. Compressive creep characteristics of extruded ultrahigh-molecular-weight polyethylene. Journal of

Biomedical Materials Research. 1998a;39:261-5.

[53] Williams, David A. Knox, Matthew G. Teeter, Holdsworth DW, Mihalko WM. Evidence that in vivo wear damage alters kinematics and contact stresses in a total knee replacement. Journal of Long-Term Effects of Medical Implants. 2010;20:43-8.

[54] Brockett CL, Abdelgaied A, Haythornthwaite T, Hardaker C, Fisher J, Jennings LM. The influence of simulator input conditions on the wear of total knee replacements: An experimental and computational study. Proc Inst Mech Eng H. 2016;230:429-39.

[55] M Kop A, Swarts E. Quantification of polyethylene degradation in mobile bearing knees: A retrieval analysis of the Anterior-Posterior-Glide (APG) and Rotating Platform (RP) Low Contact Stress (LCS) knee. Acta Orthopaedica. 2007;78:364-70.
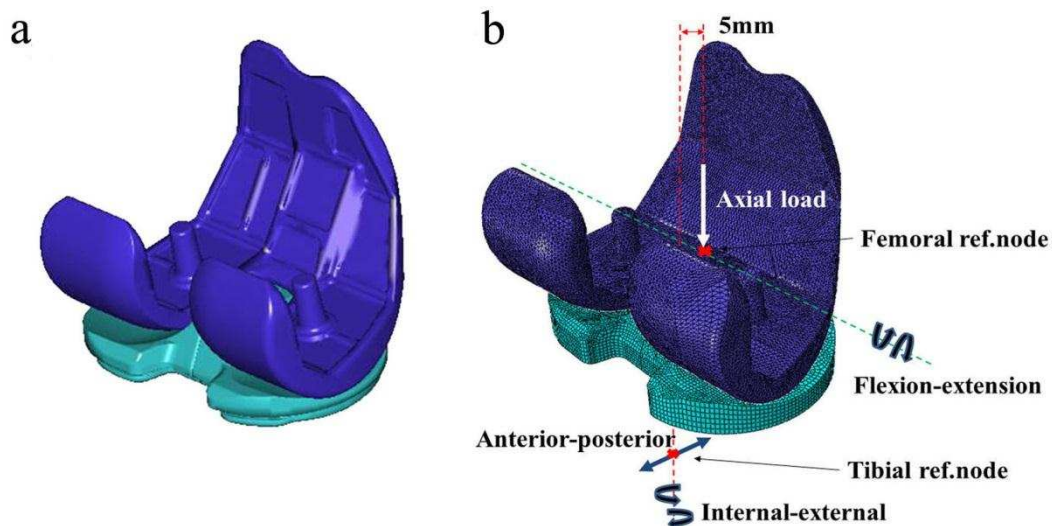
Fig.1. Patient-specific TKR model (Zimmer NK-II cruciate-retaining): femur and tibial insert solid model (a), FE model with BCs (b).
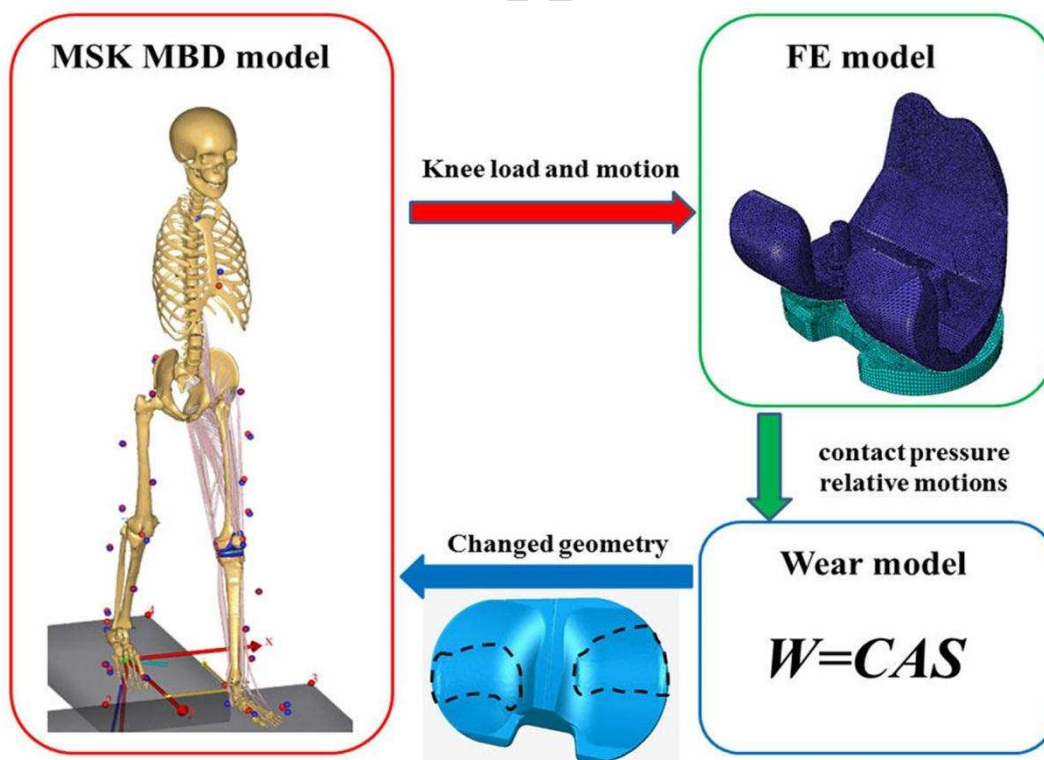
Fig.2. Novel computational framework: coupled patient-specific MSK MBD model, FE model and wear model of TKR.

13
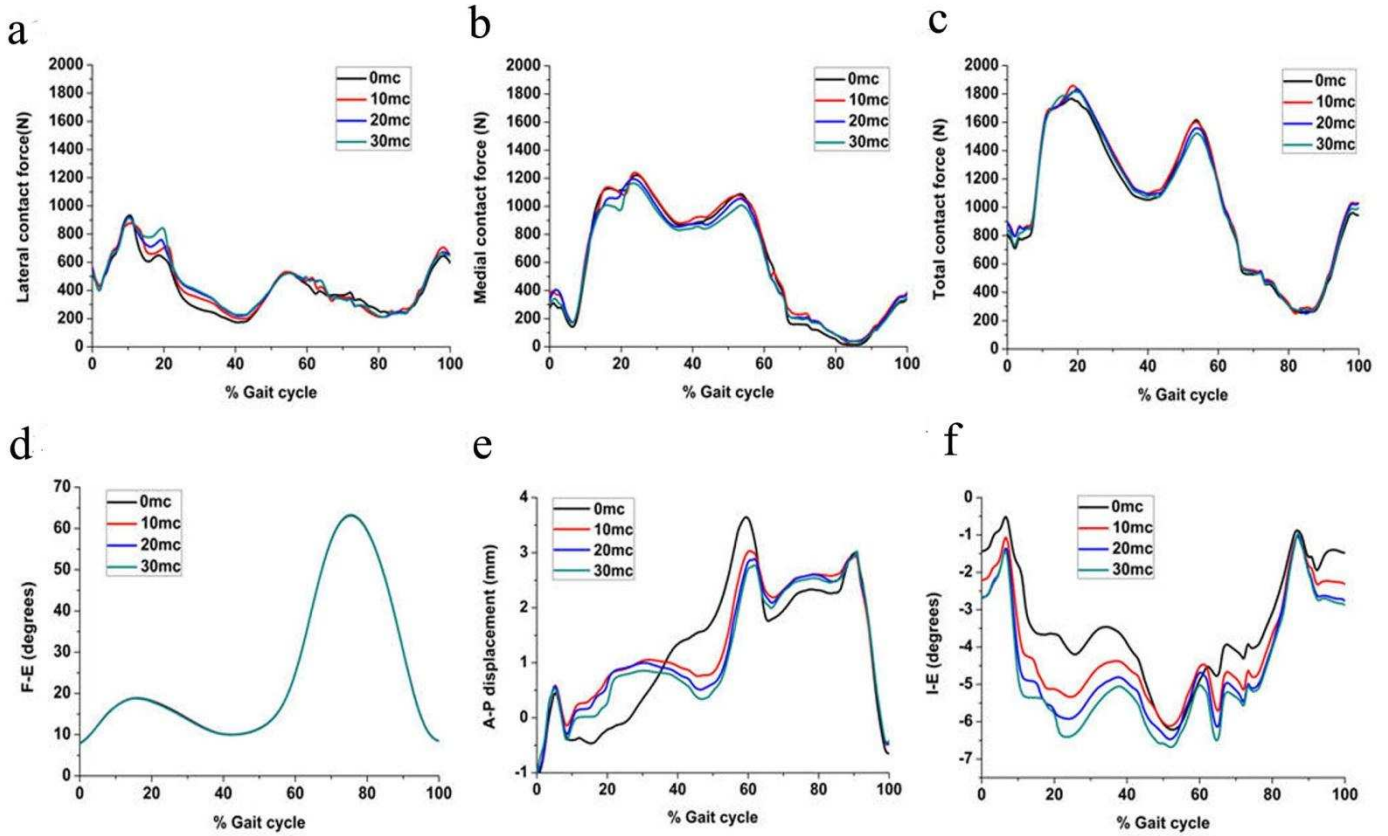
Fig.3. Contact force and motions of MSK MBD model at different simulation cycles: TF lateral contact forces (a), medial contact forces (b), total contact forces (c), femoral flexion-extension angle (d), anterior-posterior translation (e), internal-external rotation (f).
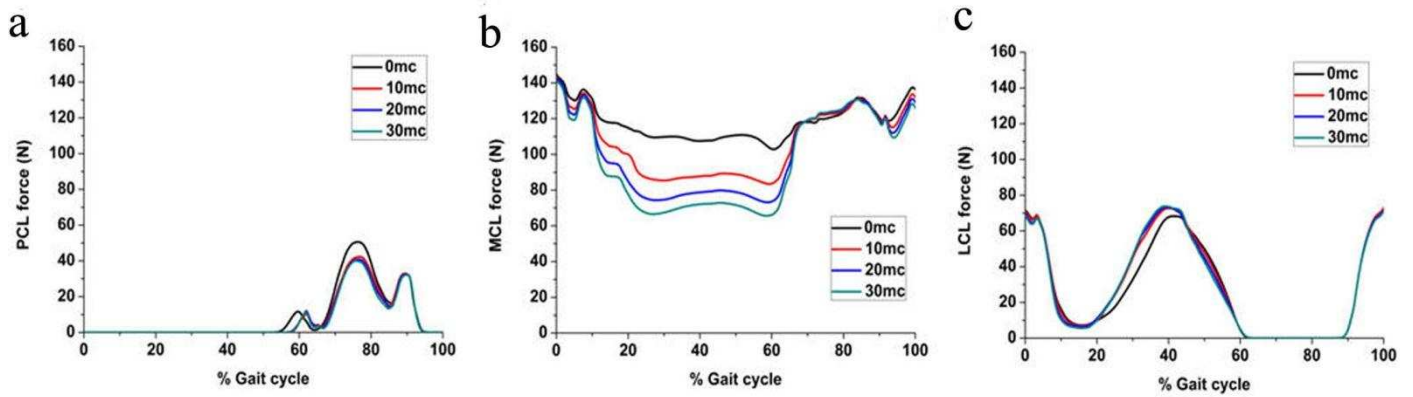

Fig.4. Ligament forces of MSK MBD model at different simulation cycles: PCL forces (a), MCL forces (b), LCL forces (c).
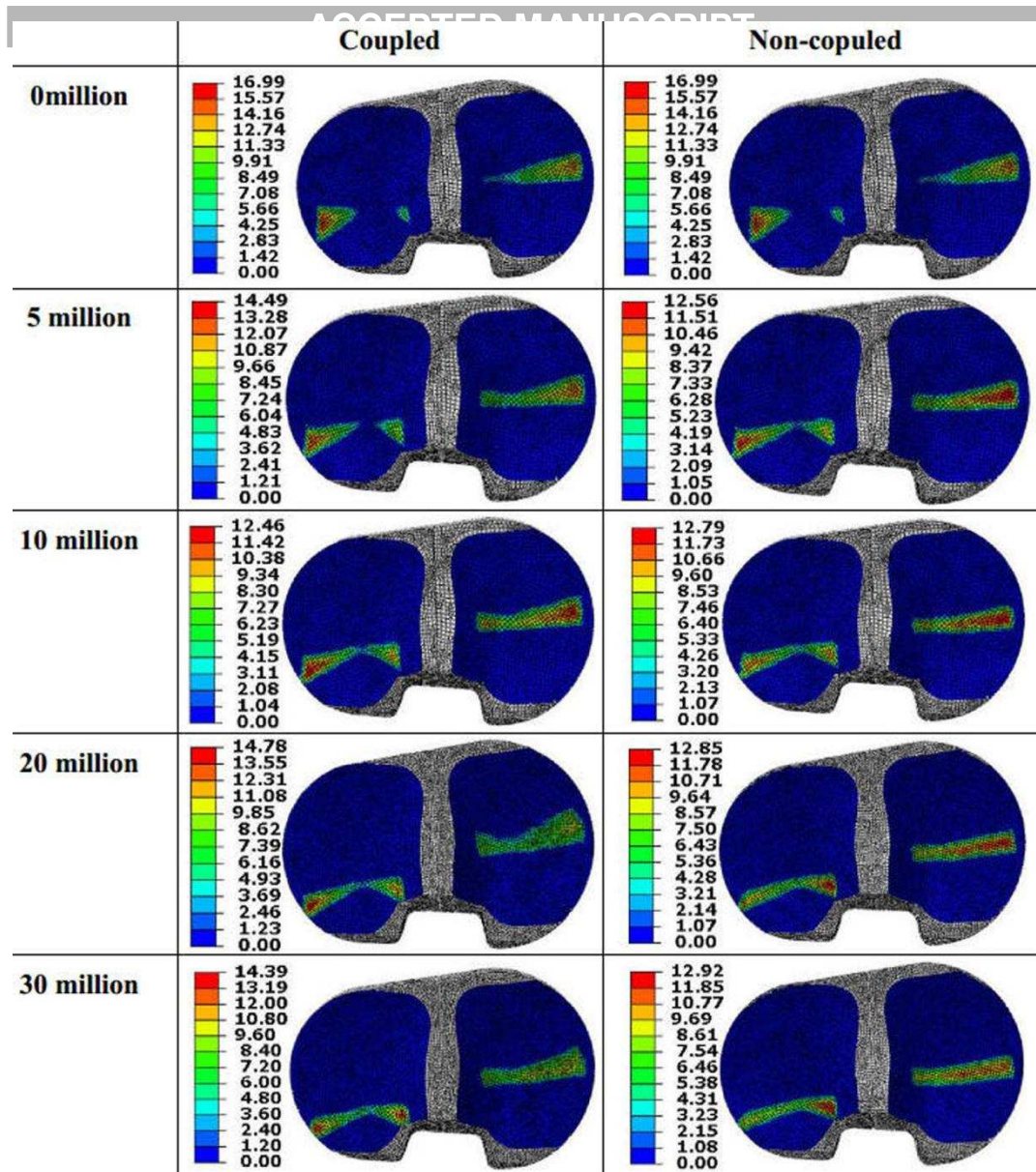
Fig.5. Contact pressure distribution (MPa) from the coupled and non-coupled models, 0 million cycles, 5 million cycles, 10 million cycles, 20 million cycles and 30 million cycles, at the moment of the maximum loading of the gait cycle.
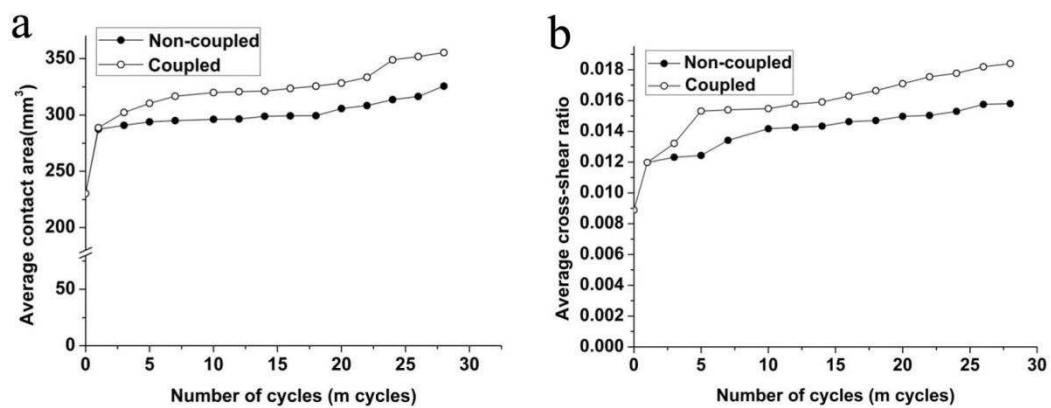

Fig.6. Average contact area (a) and average cross-shear ratio (b) from wear prediction for coupled and non-coupled models at different wear stages.
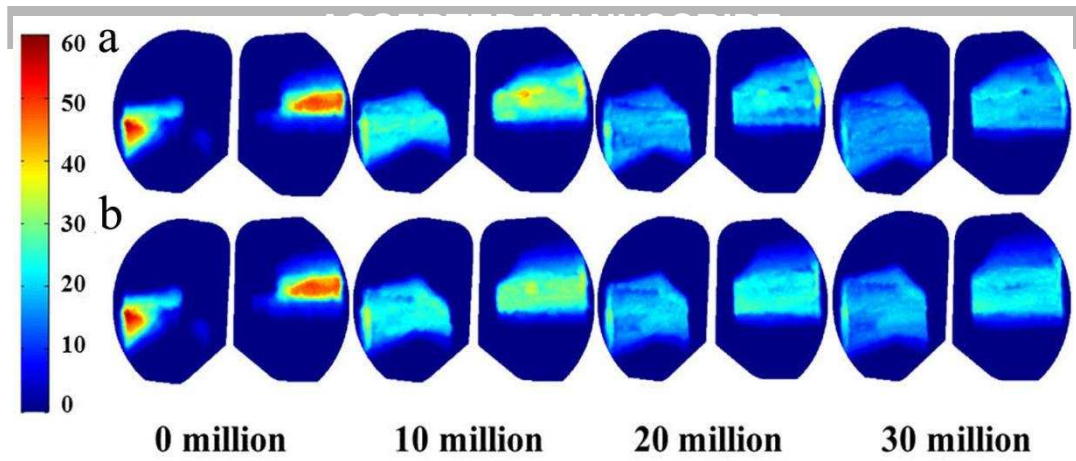
Fig.7. The accumulated sliding distance (mm) distribution of insert surface for coupled model (a) and non-coupled model (b) at different wear stages.
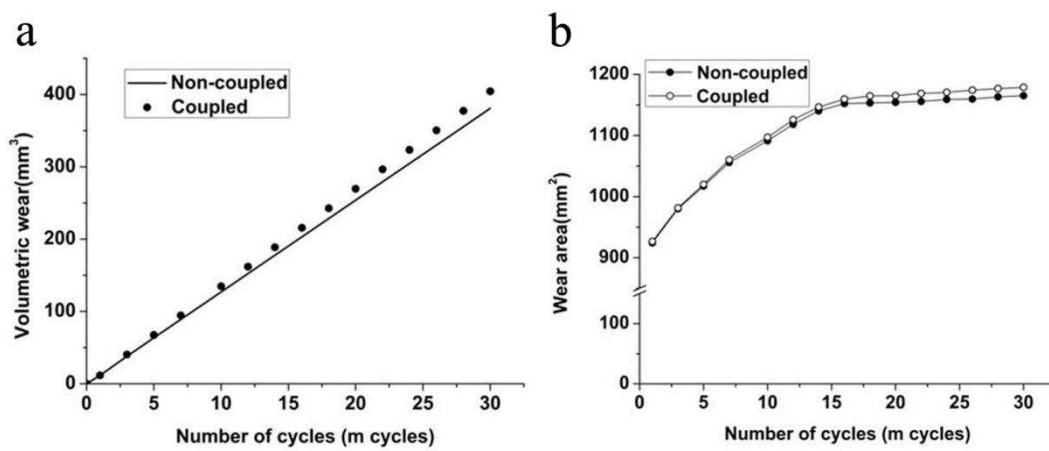

Fig.8. The volumetric wear (a) and wear area (b) of coupled and non-coupled models at different wear stages.
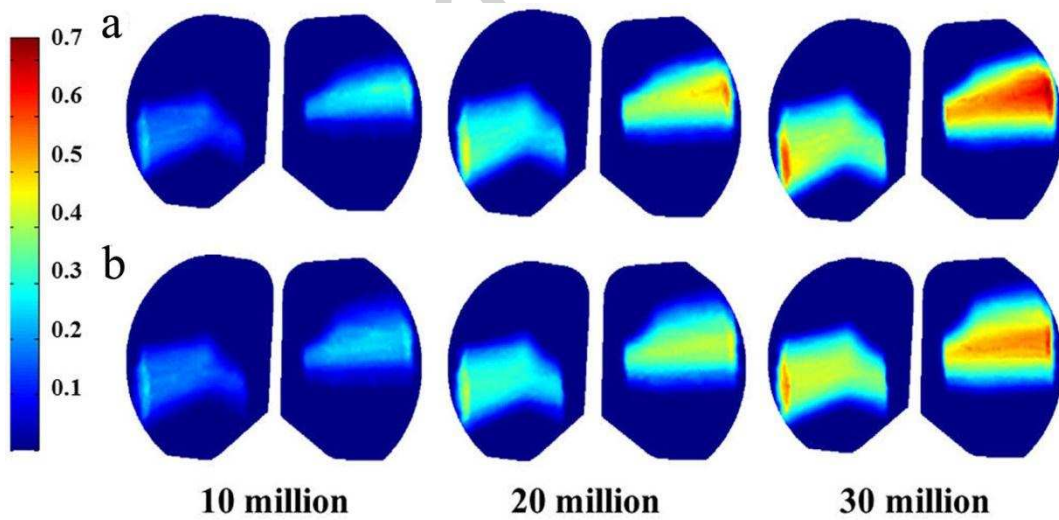

Fig.9. Linear wear (mm) distribution of the insert surface for coupled model (a) and non-coupled model (b) at different wear stages.

Highlights

- A novel patient-specific wear prediction framework was developed
- Coupling a patient-specific musculoskeletal model and finite element wear model
- Knee loads and motions were influenced by the tibial insert wear
- Varied knee contact mechanics further aggravated the tibial insert wear